ESCAP/WMO
Typhoon Committee

Available online at www.sciencedirect.com

ScienceDirect

Tropical Cyclone Research and Review 12 (2023) 200–215

www.keaipublishing.com/tcrr

A review of recent research progress on the effect of external influences on tropical cyclone intensity change

Joshua B. Wadler [a], Johna E. Rudzin [b], Benjamin Jaimes de la Cruz [c], Jie Chen [d], Michael Fischer [e], Guanghua Chen [f], Nannan Qin [g], Brian Tang [h], Qingqing Li [i,*]

[a] *Embry-Riddle Aeronautical University, Department of Applied Aviation Sciences, Daytona Beach, FL, USA*
[b] *Mississippi State University, Department of Geosciences, Starkville, MS, USA*
[c] *University of Miami, Department of Ocean Sciences, Miami, FL, USA*
[d] *Princeton University, Atmospheric and Oceanic Sciences Program, Princeton, NJ, USA*
[e] *University of Miami, Cooperative Institute for Marine and Atmospheric Studies and NOAA, Atlantic Oceanographic and Meteorological Laboratory, Hurricane Research Division, Miami, FL, USA*
[f] *Institute of Atmospheric Physics of the Chinese Academy of Sciences, Beijing, China*
[g] *Key Laboratory of Transportation Meteorology of China Meteorological Administration, Nanjing Joint Institute for Atmospheric Sciences, Nanjing, China*
[h] *University at Albany, State University of New York, Department of Atmospheric and Environmental Sciences, Albany, NY, USA*
[i] *Nanjing University of Information and Science Technology, Nanjing, China*

Available online 12 September 2023

Abstract

Over the past four years, significant research has advanced our understanding of how external factors influence tropical cyclone (TC) intensity changes. Research on air-sea interactions shows that increasing the moisture disequilibrium is a very effective way to increase surface heat fluxes and that ocean salinity-stratification plays a non-negligible part in TC intensity change. Vertical wind shear from the environment induces vortex misalignment, which controls the onset of significant TC intensification. Blocking due to upper-level outflow from TCs can reduce the magnitude of vertical wind shear, making for TC intensification. Enhanced TC-trough interactions are vital for rapid intensification in some TC cases because of strengthened warm air advection, but upper-level troughs are found to limit TC intensification in other cases due to dry midlevel air intrusions and increased shear. Aerosol effects on TCs can be divided into direct effects involving aerosol-radiation interactions and indirect effects involving aerosol-cloud interactions. The radiation absorption by the aerosols can change the temperature profile and affect outer rainbands through changes in stability and microphysics. Sea spray and sea salt aerosols are more important in the inner region, where the aerosols increase precipitation and latent heating, promoting more intensification. For landfalling TCs, the intensity decay is initially more sensitive to surface roughness than soil moisture, and the subsequent decay is mainly due to the rapid reduction in surface moisture fluxes. These new insights further sharpen our understanding of the mechanisms by which external factors influence TC intensity changes.

Keywords: Tropical cyclone; External influence; Intensity change; Review

1. Introduction

Tropical cyclones (TCs) are not isolated atmospheric systems; various external factors can influence their development to diverse degrees. These factors include, but are not limited to, land and ocean, solar radiation, environmental vertical wind shear (VWS), ambient humidity, and other surrounding

* Corresponding author. Nanjing University of Information and Science Technology, China.
E-mail address: liqq@nuist.edu.cn (Q. Li).
Peer review under responsibility of Shanghai Typhoon Institute of China Meteorological Administration.

Production and Hosting by Elsevier on behalf of KeAi

https://doi.org/10.1016/j.tcrr.2023.09.001

atmospheric systems. Variations in these external factors and their interactions with the TC circulation complicate the physical processes underlying TC intensity changes. Therefore, understanding these factors and the corresponding interactions will contribute to a more profound understanding of the dynamics of TC intensity change and the forecasting of TC intensity. Endeavors have been longstanding to investigate how the above factors affect the change in TC intensity.

This review article summarises the major advances in external influences on TC intensity change from 2019 to 2022, based on the World Meteorological Organization's 10th International Workshop on Tropical Cyclones report. It covers the characteristics and physical processes of TC intensity change due to ocean impacts, air-sea interaction, VWS, surrounding systems, aerosols, the Saharan air layer (SAL), and radiation. In addition, more recently, a steadily rising effort has been devoted to investigating the characteristics and mechanisms of intensity changes during TC landfall. Therefore, the latest research findings on intensity changes during TC landfall are also presented here.

2. Ocean influences

A significantly clearer picture of ocean influences on TC intensity change has emerged. In addition to the classical warm ocean eddy (WOE) paradigm[1] (Leipper and Volgenau 1972; Shay et al., 2000), new perennial warm ocean regimes have been identified, and they were noted to sustain intense sea-to-air enthalpy fluxes, often leading to phases of rapid intensification (RI; greater than 30 kt increase in intensity over 24 h) in TCs. The role of strong horizontal gradients in sea surface temperature (SST) in enhancing the fluxes during RI —presumably due to higher SSTs on the warm side of the gradient— and causing rapid weakening (RW) of TCs over cooler SSTs was also observed.

2.1. Perennial warm ocean regimes

A persistent warm coastal regime was noted during Hurricane Harvey (2017) in the Gulf of Mexico. An analysis found that, at the time of landfall, the Texas Bight was well mixed with very warm water extending from the surface to bottom—mixing induced by Harvey had a small impact on SSTs which remained high and supported continued intensification (Potter et al., 2019).

Much knowledge has been attained regarding the interaction of TCs with salinity-stratified upper ocean waters and how they affect ocean mixing, air-sea fluxes, and TC intensification. Rudzin et al. (2019, 2020) revealed the influence the Amazon-Orinoco River plume had on the RI of Hurricane Irma, which was promoted by more favorable oceanic conditions, air-sea fluxes, and atmospheric boundary layer conditions over the salinity-stratified river plume compared to those before RI when the TC was not over the river plume. Furthermore, Hlywiak and Nolan (2019) found that the intensification of TCs of at least minimal hurricane status was supported by a barrier layer (a vertical salinity gradient in the ocean temperature mixed layer), whereas the intensification of weaker TCs was hindered. Balaguru et al. (2020a,b) confirmed numerical evidence from Hlywiak and Nolan (2019) by showing that specific locations and intensification thresholds for which salinity-stratification becomes important in forecasting RI. They also statistically link salinity-stratified upper ocean conditions with RI events of TCs (Fig. 1).

2.2. SST gradients

An observational study covering 913 TC cases over the western North Pacific from 1988 to 2017 found that the RW cases occurred in regions with a stronger meridional SST gradient and cooler SSTs (Ma et al., 2019). The weakening rate and the RW number significantly increased over the region of 25°N–35°N, 120°E–150°E from 1982 to 2000 to 2001–2019—stronger SST gradients were observed in this region in recent years, presumably caused by inhomogeneous Pacific warming (Song et al., 2020).

2.3. Air-sea flux

A new perspective on the bulk aerodynamic formulae was introduced to evaluate the relative contribution of wind-driven (U10) and thermodynamically-driven (ΔT and Δq) ocean heat-uptake, where U10 is 10-m wind speed, and ΔT and Δq are air-sea temperature and moisture differences, respectively (Jaimes de la Cruz et al., 2021). Compensation in air-sea moisture flux by larger values of Δq at moderate values of U10 led to intense inner-core moisture fluxes >600 W m^{-2} during RI. Peak values in Δq preferentially occurred over oceanic regimes with higher SST and upper-ocean heat content. Jaimes de la Cruz et al. (2021) study indicates that increasing SST and Δq is a very effective way to increase surface heat fluxes—this can be easily achieved as a TC moves over perennial warm ocean regimes. These results call for new TC intensification paradigms and accurate measurement and representation of Δq in numerical models to better predict RI events.

2.4. Boundary layer and air-sea coupling

Wadler et al. (2021) was the first observational study of Hurricane Michael (2018) to relate the distribution of air-sea enthalpy fluxes over mesoscale oceanic eddy features to the known asymmetries in storm structure imposed by environmental wind shear. This study reported that Hurricane Michael interacted with an oceanic eddy field leading to cross-storm SST gradients of ~2.5 °C (Fig. 2b). This led to the highest enthalpy fluxes occurring left of shear, favoring the sustainment of updrafts into the upshear quadrants and a quick recovery from low-entropy downdraft air. Similarly, Rudzin et al. (2020) identified that the recovery of the boundary layer during

[1] Warm ocean regimes that do not cool much and SSTs remain well above the 26 °C threshold during the storm, which facilitates rapid intensification of TCs.

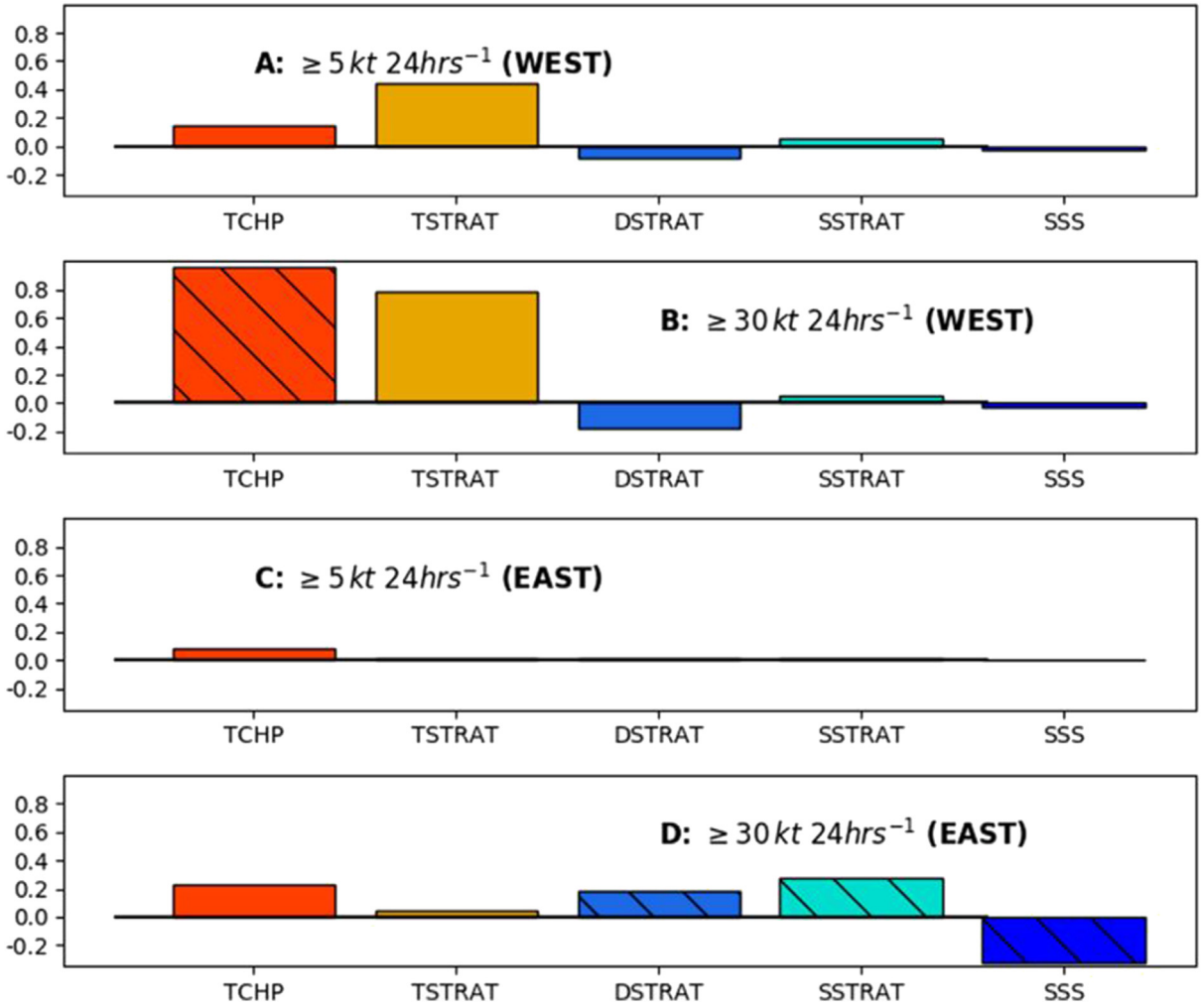

Fig. 1. Along-track anomalous mean tropical cyclone heat potential (TCHP; 10 kJ cm^{-2}), temperature stratification (TSTRAT; °C), density stratification (DSTRAT; kg m^{-3}), salinity stratification (SSTRAT; psu), and sea surface salinity (psu) in the tropical Pacific (WEST; a,b) and tropical Atlantic (EAST; c,d) for cases where the 24-h intensity change is greater than or equal to 5 kt (a,c) and RI (b,d). The western region corresponds to 10°–30°N, 70°–100°W, and the eastern region corresponds to 10°–30°N, 40°–70°W. Data is extracted from HYCOM. Figure from Balaguru et al. (2020a,b) showing that salinity stratification plays an equal, if not more important, role compared to TCHP in air-sea interactions in tropical Atlantic RI, whereas TCHP and temperature stratification dominate air-sea interactions during RI in the tropical Pacific.

Hurricane Irma (2017)'s RI was supported by a favorable SST response due to a salinity-stratified upper ocean from the Amazon-Orinoco River plume. In the numerical study by Kumar et al. (2021), the influence of boundary-layer dynamics and air-sea coupling on the change in the location of the eye-wall updraught and the intensity of a mature tropical cyclone was investigated in a simulation of a TC run with the fully coupled ICOsahedral Nonhydrostatic (ICON) model in a global configuration. Results show that boundary-layer dynamics should be incorporated into any explanation of TC intensity change in response to sea surface cooling in coupled atmosphere-ocean models with a realistic ocean-eddy field (Fig. 3; Kumar et al., 2021).

2.5. Ocean waves

A new relationship between waves and TC intensity change was recently indicated. Zhang and Oey (2019) utilized satellite significant wave height, a parametric TC model, and NCEP one-degree reanalysis fields; they found a spatial pattern in the TC field that relates significant wave height to low-level moisture convergence in rapidly-intensifying and non-rapidly-intensifying TCs. In rapidly intensifying TCs, young waves appear in the right-front quadrant, and the low-level moisture flux convergence is symmetrical throughout the storm's inner-core region, presumably due to the combined effect of wind-driven advection of moisture, near-surface wind speed intensification, and forward storm motion.

2.6. New and updates to observational platforms

Progress in ocean observing in TC environments has led to new knowledge in understanding air-sea interaction during and after TC passage. Domingues et al. (2019) provide an overview of ocean observing advances to support TC research and prediction. Autonomous ocean vehicles, such as ocean gliders,

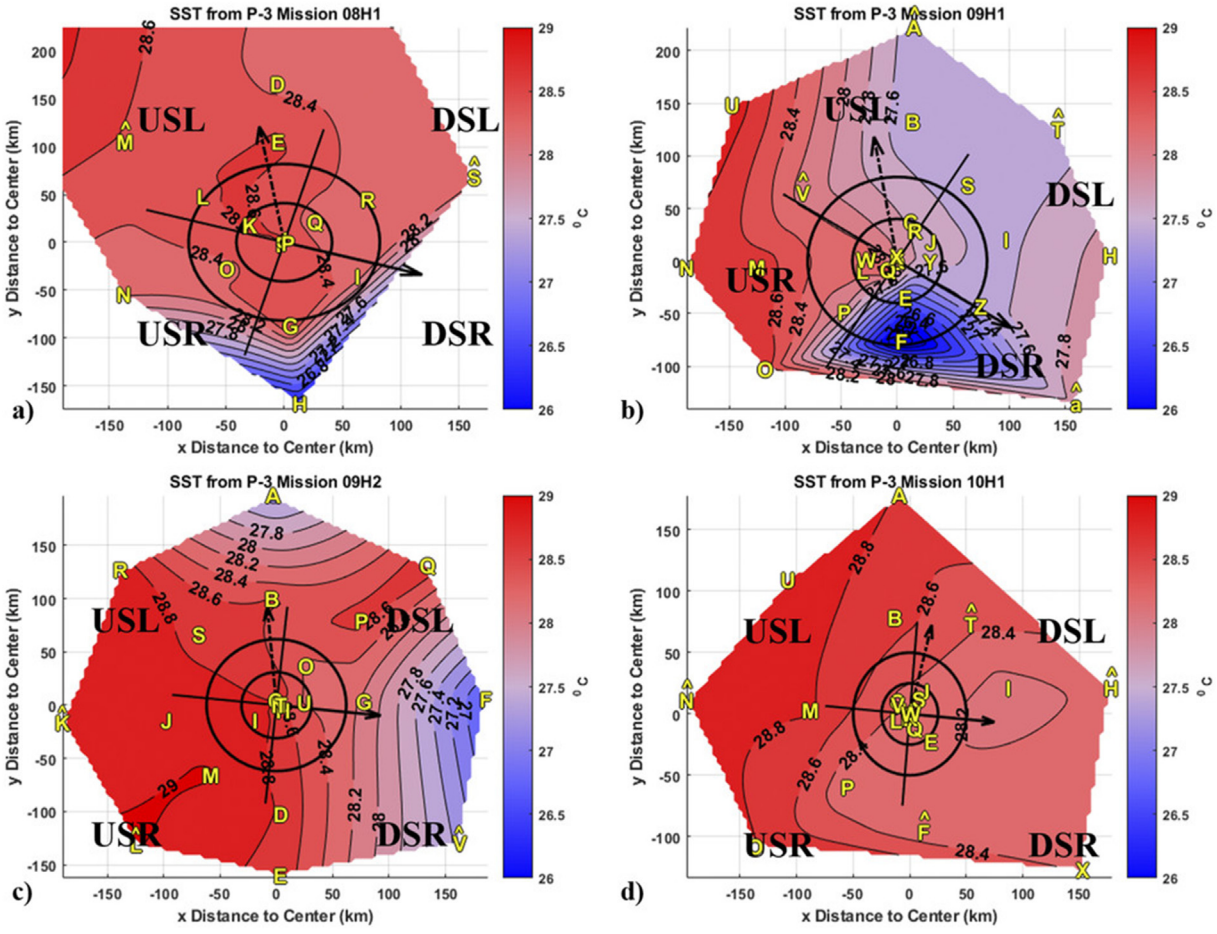

Fig. 2. SST variability during the rapid intensification of category-5 Hurricane Michael (2018)from aircraft expendable ocean profilers. The solid black (dashed black) arrow from the center represents the shear (motion) vector. Solid black lines from the storm center outline the shear-relative quadrants: down-shear right (DSR), down-shear left (DSL), up-shear left (USL), and up-shear right (USR). From Fig. 8 of Wadler et al. (2021a,b).

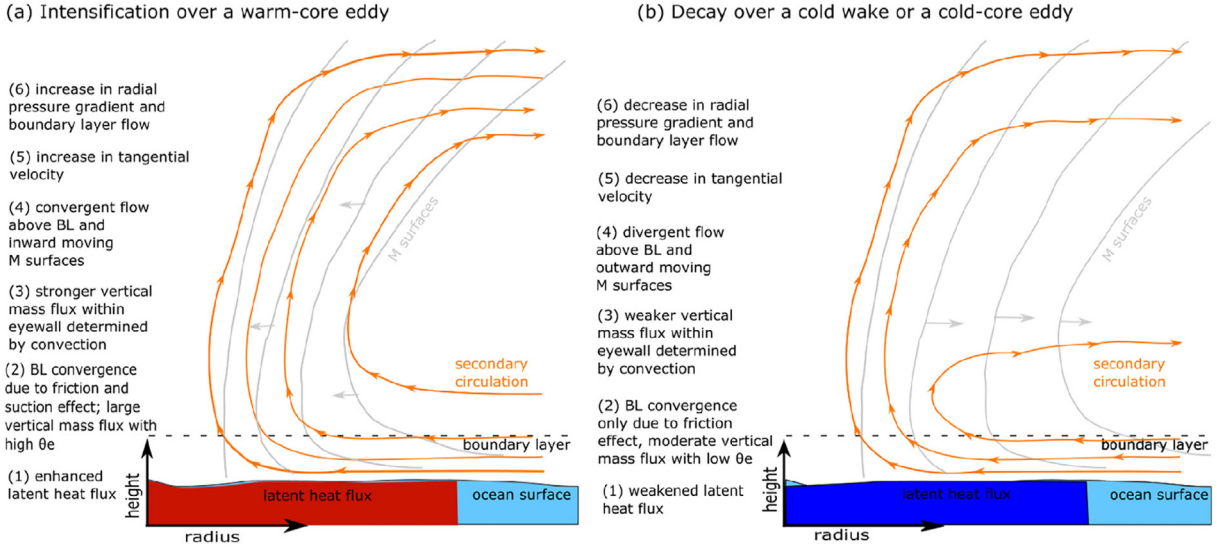

Fig. 3. Conceptual models of TC intensification and decay about underlying ocean features. (a) Intensification over the WOE. (b) Decay or weakening over the storm's cool wake or a cool mesoscale cyclone. From Fig. 1 of Kumar et al. (2021).

electromagnetic autonomous profiling explorer (EM-APEX) floats, and Saildrones, are technology in the TC community used to diagnose upper ocean and air-sea characteristics before, during, and after TC passage. Underwater gliders have been running operationally through the US Integrated Ocean Observing Systems Program since 2014 and were included in the NOAA Hurricane Field Program starting in 2018. The multi-institution fleet of gliders has since collected ~600,000 profiles during the 2018–2021 Atlantic Hurricane Seasons (Miles et al., 2021). Observations collected by gliders have been shown to improve the pre-storm representation of the ocean and provide better TC intensity forecasts in coupled forecast models than those that do not ingest the data.

Simultaneous measurements of ocean current (including vertical shear), temperature, and salinity are possible with the EM-APEX float (Shay et al., 2019). Measurements of vertical shear over the upper ocean from this and other platforms–potentially Saildrones–can guide the improvement of the parameterization of vertical mixing in the ocean component of coupled TC forecast models. Elucidating the role of vertical mixing within the upper ocean is critical for better understanding sea surface cooling and ensuing air-sea heat fluxes and TC intensity change.

3. Impacts of vertical wind shear

VWS, typically defined as the vector difference in the environmental wind between 850 and 200 hPa, has been shown to have significant impacts on TC structure and intensity change. The effects of VWS on the TC circulation are largely unfavorable, as VWS tends to tilt the vortex in the vertical (DeMaria 1996; Boehm and Bell 2021), ventilate the TC warm core (Tang and Emanuel 2010; Alland et al. 2021a, b; Wadler et al., 2021), and decrease the symmetry and areal coverage of diabatic heating associated with convective processes (Nolan et al., 2007; Alland et al. 2021a, b). If shear-driven ventilation is too strong, idealized numerical modeling studies have shown TC development fails to occur at all (Alland et al., 2021a). Alternatively, environments of moderate VWS exhibit a wide range of TC intensity changes, ranging from weakening to rapid intensification (RI; e.g., Alvey et al., 2020; Hazelton et al., 2020; Finocchio and Rios-Berrios 2021). Consequently, recent work has focused on better understanding the processes associated with the rate of TC intensity change in such environments.

3.1. Vortex tilt induced by VWS

A common research theme over the past four years has been the effects of VWS on the vortex tilt structure. At a base level, VWS acts to advect differentially, or tilt, the TC vortex toward the downshear direction. A tilted TC vortex induces a balanced azimuthal wavenumber-1 response, where a cold anomaly develops in the downtilt region of the storm, co-located with regions of strong convection, whereas a warm anomaly is found in the uptilt portion of the TC (Boehm and Bell 2021). In relatively weak TCs (i.e., those below hurricane intensity; maximum sustained 10-m wind <33 m s^{-1}), which feature a wider range of tilt magnitudes than TCs of hurricane intensity (Fischer et al., 2022), the onset of more rapid rates of TC intensification is closely related to the transition of a misaligned vortex toward alignment (e.g., Ryglicki et al., 2019; Chen et al., 2019b; Tao and Zhang 2019; Alvey et al., 2020; Rios-Berrios et al. 2020; Rogers et al., 2020; Schecter and Menelaou 2020; Schecter 2022). However, a completely aligned vortex does not appear to be a requirement for RI (e.g., Alvey et al., 2022), and the degree of tilt reduction needed for faster rates of TC intensification to be realized has been shown to display sensitivity to environmental conditions, such as the sea surface temperature (e.g., Schecter 2022). Additionally, the vertical structure of the shear direction has also been found to affect the vortex tilt and TC intensity evolution, with a clockwise turning hodograph found to be favorable for quicker vortex alignment and intensification (Gu et al., 2019).

3.2. Ventilation

The relationship between the TC vortex tilt structure and VWS can strongly influence the degree of ventilation a TC experiences (e.g., Chen et al., 2019b). Recent work has divided ventilation into radial and downdraft pathways (Alland et al. 2021a; 2021b; 2022). Radial ventilation acts in two ways. At upper levels (5–9 km altitude), radial ventilation is closely linked to the vortex tilt structure, as the misaligned TC circulation acts to transport relatively low-equivalent potential temperature air (θ_e) from the TC environment toward the TC center in the upshear and right-of-shear quadrants of the storm (Fig. 4b). At lower levels (0–3 km altitude), radial ventilation acts similarly to downdraft ventilation, transporting low θ_e air to the inflow layer via convective downdrafts in the downshear and left-of-shear quadrants of the storm (Fig. 4a,c).

When low-θ_e air is transported to the boundary layer, it can recover via air-sea enthalpy fluxes before reaching the eyewall. Recent work has shown that boundary layer recovery of low-θ_e air is a function of height such that most parcels fully recover (no θ_e deficit in the eyewall) near the sea surface. In contrast, the most destructive area for downdraft ventilation is near the top of the inflow layer, where low-θ_e air can be transported inwards toward the eyewall and is too high to be affected by the air-sea enthalpy fluxes (Wadler et al., 2021b). The effects of downdraft ventilation can also be mitigated by the inclusion of radiation which can change the stability profile (Rios-Berrios 2020), the presence of a high-θ_e layer above the inflow layer which can act as a thermodynamic shield (Wadler et al., 2021a,b), and higher sea surface temperatures (Chen et al., 2021b). Through a composite analysis of dropsonde observations, Nguyen et al. (2019) showed that TCs undergoing intensification tend to have higher air-sea enthalpy fluxes than non-intensifying TCs, especially in the upshear quadrants, indicative of more effective recovery from ventilation.

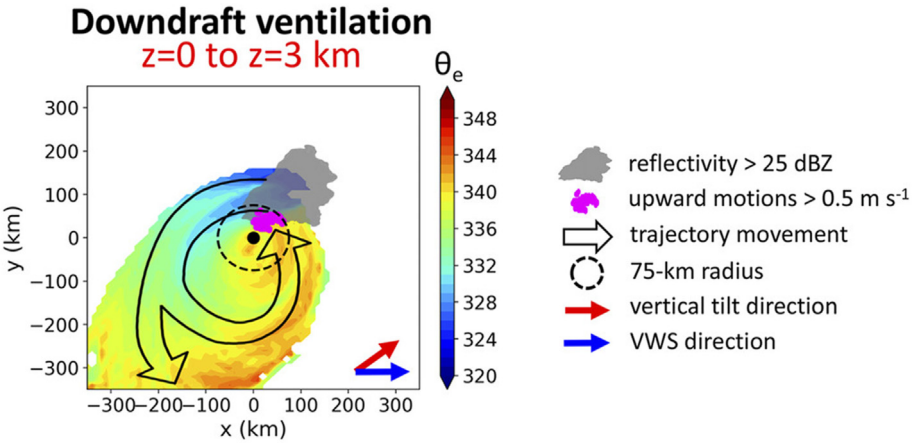

Fig. 4. Conceptual model adapted from Alland et al. (2021a and 2021b) of radial ventilation. In shading, (a) the average equivalent potential temperature (K) of trajectories initialized in radial ventilation regions between heights of 0 and 3 km, (b) the average RH (%) of trajectories initialized in radial ventilation regions between heights of 5 and 9 km and (c) the average equivalent potential temperature of trajectories initialized in downdraft ventilation. Other information includes reflectivity greater than 25 dBZ (gray shading), upward motions greater than 0.5 m s^{-1} (magenta dots), the TC center averaged between heights of 5 and 9 km (white ×), parcel movement (black arrows), the inner 75 km (dashed circle), the vertical tilt direction from the surface to 6 km (red arrow), and the VWS direction (blue arrow).

3.3. Sensitivity to TC intensity and structure

The intensity response of a TC to VWS is also a function of TC intensity and vortex structure. When VWS is imposed on a weak tropical storm, it can decouple the vortex, which disallows intensification (Fig. 5; Finocchio and Rios-Berrios 2021). When VWS is imposed on TCs of hurricane strength, the intensity response of the storm is sensitive to the radial vortex structure. Finocchio and Rios-Berrios (2021) found that simulated TCs which were subject to increasing VWS in the midst of a period of RI, or those had recently completed RI, were prone to lateral ventilation, which can reduce the TC's inner-core θ_e, due in part to their narrower vortex structures and limited inertial stability in the outer core. Alternatively, when VWS was imposed on mature TCs following a period of RI, which had broader vortex wind fields, these storms were more resilient to the potentially harmful effects of ventilation and exhibited a larger steady-state intensity.

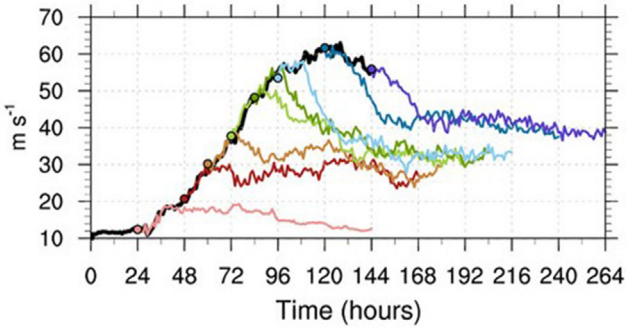

Fig. 5. Times series from Fig. 2c of Finocchio and Rios-Berrios (2021) of maximum azimuthally averaged 10-m wind speed. The baseline simulation is in black, and the colored circle markers are when shear begins to increase to 15 m s^{-1} for each simulation.

3.4. Sensitivity to VWS properties

Recent work has also focused on how nuanced properties of the flow impact TC intensity change. For example, outside of the deep tropics, TCs experiencing VWS with a northerly component tend to have more symmetric boundary layer thermodynamic distributions than TCs experiencing VWS with a southerly component (Wadler et al., 2022). Additionally, the direction of the low-level flow relative to the shear direction has been shown to affect the rate of TC intensity change due to its influence on the spatial pattern of surface fluxes. For example, Lee et al. (2021) found through a set of idealized simulations that TCs with an upshear-left directed low-level flow intensified at greater rates than TCs with a downshear-right directed low-level flow; however, Chen et al. (2019a) found a downshear-left directed low-level flow yielded the greatest rates of TC intensification using a different modeling set up, which imposed the motion-relative shear asymmetries on weaker TCs using a different shear profile than Lee et al. (2021). An analysis of observed TCs by Chen et al. (2021a) concluded a downshear-left directed low-level flow is the most favorable for TC intensification, whereas an upshear-right oriented low-level flow yields TCs that instead more quickly grow in size.

3.5. Effects of the TC circulation on environmental VWS

Other studies have highlighted an intensification pathway through which a TC can locally modify the environmental flow. Using idealized simulations, Ryglicki et al. (2019, 2020) demonstrated how convectively driven divergent upper-level outflow associated with a tilted vortex can act against background environmental flow, as shown schematically in Fig. 6. If the vertical structure of the environmental shear is peaked in the upper troposphere, this outflow blocking mechanism can

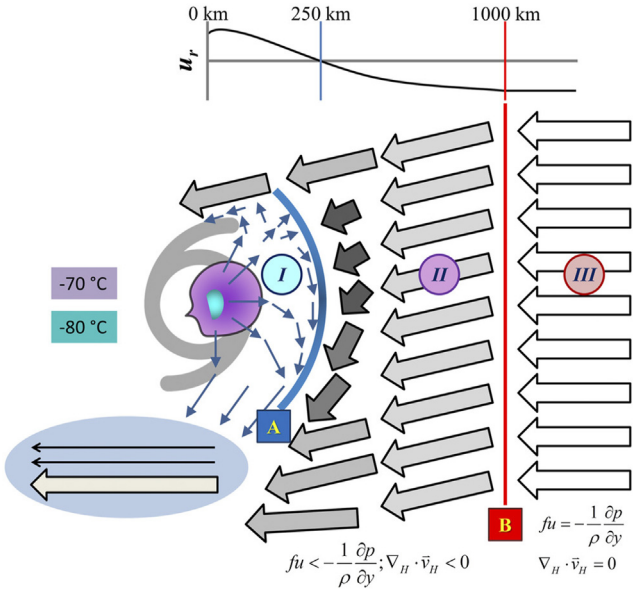

Fig. 6. Schematic illustrating the outflow of a TC that distorts the environmental winds. Large thick arrows are environmental flow; thin arrows are TC outflow. Outlines of lavender and teal colors indicate satellite imagery. The blue-shaded oval is the outflow jet. The letters (A and B) and roman numerals (I, II, and III) indicate the various boundaries and regions, respectively. Region I is strictly the outflow, and it is defined as having a density lower than that of the surrounding atmosphere at a given level. A is the outflow front, where the outflow and the environment collide. Beyond the outflow front lies Region II, where the environmental winds become subgeostrophic, decelerate, converge, slowly sink, and turn to the left. B indicates the bow wave, which is the farthest boundary where the outflow affects the environmental winds. Region III is the unaffected free atmosphere in geostrophic thermal wind balance. Spatially, radially from the core, A exists approximately 200–250 km upshear, and B exists approximately 1000 km upshear. The top line is radial wind at different radii. The shear vector is coincident with environmental winds (easterly). From Fig. 2 of Ryglicki et al. (2019).

result in a pocket of relatively weak VWS, which is favorable for TC intensification. An example of this "atypical rapid intensification" pathway was examined using satellite and airborne Doppler radar observations of Hurricane Dorian (2019; Ryglicki et al., (2021). Other studies using larger sample sizes have also supported the significance of outflow blocking, locally reducing the vertical wind shear and promoting TC intensification. For example, by examining a reanalysis data set and infrared satellite observations, Shi and Chen (2021) found that RI cases in environments of moderate and strong vertical wind shear (defined as shear magnitudes between 4.5 and 11 m s^{-1} and >11 m s^{-1}, respectively) were associated with an increase in upshear convection and upper-level outflow in the 24 h before RI onset, leading to a decrease in local VWS (defined as shear calculated within the innermost 200 km of the TC). Additionally, Shi and Chen (2021) found that in storms experiencing moderate-to-strong environmental vertical wind shear, TC intensity change was more closely correlated with the local wind shear magnitude than the environmental, synoptic-scale wind shear magnitude. Similarly, Dai et al. (2021) used idealized simulations to show how TC intensity change is linked to the "TC-induced shear difference" (TCSD), which is defined as the difference between the environmental shear and the shear computed within the innermost 500 km of the TC. It was hypothesized that the TCSD results from convectively-driven asymmetric TC outflow, and when the TCSD is oriented upshear, the TC is situated in a more favorable local environment for intensification.

4. Interactions between a TC and surrounding systems

4.1. Interactions with upper-level troughs and lows

Upper-level troughs can provide unique forcing for convection that favors TC intensification. Qiu et al. (2020) examined the eddy flux convergence (EFC) characteristics and concluded that the enhanced TC-trough interaction by the large-scale circulation pattern was critical for the offshore RI of several TCs, even under larger VWS. An observational study of Hurricane Michael (2018) showed that the intensification of this hurricane was attributed to dominant warm air advection linked to a vertically-deep trough during its landfall near Mexico (Callaghan 2019). Moreover, a TC-trough interaction can lead to additional low-level inflow and upper-level outflow, as shown in the RI of Hurricane Helene (2006) (Qin and Wu 2021). Yan et al. (2021) indicated that the upper-tropospheric cold low (UTCL) contributed to the intensification of Typhoon Jongdari (2018) by enhancing the EFC, reducing the inertial stability, and enhancing the upper-level divergence of the absolute angular momentum flux.

The upper-level troughs can also impede TC intensification since they tend to be associated with unfavorable environmental conditions. Hurricane Dennis (2005) weakened due to the strong cold air advection over its western part when interacting with an upper-level trough (Callaghan 2019). Yue et al. (2020) also found that, for weakening TCs, low-tropospheric cold air was to the northwest of the TCs associated with upper-level troughs.

The upper-tropospheric trough morphology may be responsible for the different intensity changes during TC-trough interactions. Fischer et al. (2019) used machine learning to identify three unique clusters of TC–trough configurations. It was found that TCs in the cutoff cluster consisted of a larger intensification rate than those in the northwest and northeast trough clusters, and RI tended to be associated with upper-level troughs with a shorter zonal wavelength and a greater upstream TC-trough displacement.

4.2. Monsoon gyre and trough influences

Monsoon gyres and troughs can cause striking TC intensity changes when interacting with TCs (Yan et al., 2019; Qiu et al., 2020; Yang et al. 2022). The climatological monsoon trough that transports moist air into TCs is responsible for the offshore TC RI in large environmental VWS over the South China Sea (Qiu et al., 2020). Wu et al. (2020) indicated that low-level convergence and vorticity in the inner-core region of TCs could be enhanced when TCs approach the monsoon trough. However, TCs does not always intensify when interacting with monsoon gyres and troughs. Yan et al. (2019) indicated that the intensification rate for a TC embedded in a monsoon gyre was slower than without background flow, possibly because of larger outer-core size, increased asymmetric perturbations, and up-shear tilting.

4.3. Binary TC interactions

Complete merger, partial merger, complete straining-out, partial straining-out, and elastic interaction are typical interactions between TCs (Fig. 7; Liou and Pandey 2020). Liou and Pandey (2020) found that a weaker TC could be partially strengthened by a stronger one when a strong interaction occurs between them. However, in the case of TCs Kulap and Noru (2017), the binary interaction suppressed the intensification of Noru because of moisture cutoff and enhanced VWS (Li and Ge 2021). Furthermore, from a view of idealized modeling, Liu et al. (2021) demonstrated that ventilation of the warm upper-level core of one TC could be produced by VWS induced by the upper-level anticyclone of the other TC, leading to a weakening of the former TC.

5. Effects of other environmental factors

5.1. Aerosol impacts

Aerosol effects on TCs can be divided into direct effects (aerosol-radiation interactions) and indirect effects (aerosol-cloud interactions). Direct effects of anthropogenic aerosols and dust may be more important in the outer region (Liang et al., 2021b; Shi et al., 2021) (Fig. 8), affecting rainbands through changes in stability and microphysics. In contrast, indirect effects due to sea spray and sea-salt aerosols may be more important in the inner region (Fig. 8), where increases in cloud ice, precipitation, latent heating, and vertical velocity could promote more intensification (Jiang et al., 2019; Luo et al., 2019; Shpund et al., 2019; Shi et al., 2021).

It appears uncertain what the net aerosol effect is on TC intensity due to the complicated interactions between aerosols, radiation, and microphysics. Shi et al. (2021) found that greater aerosol concentrations lowered the intensity in simulations of Hurricane Nadine (2012). On the other hand, Cotton and Walko (2021a) found that an environment with ten times the aerosol concentration resulted in a more intense simulation of Hurricane Harvey (2017) due to the "condensational invigoration mechanism" (Cotton and Walko 2021b). Thus, aerosol effects are likely dependent on the TC lifecycle stage, types of aerosols, and other aspects of the environment.

5.2. Sarahan air layer

The SAL affects TCs in the North Atlantic through its dust concentrations and dry (low-θ_e) air; however, there are still questions concerning the degree of the impediment to TC

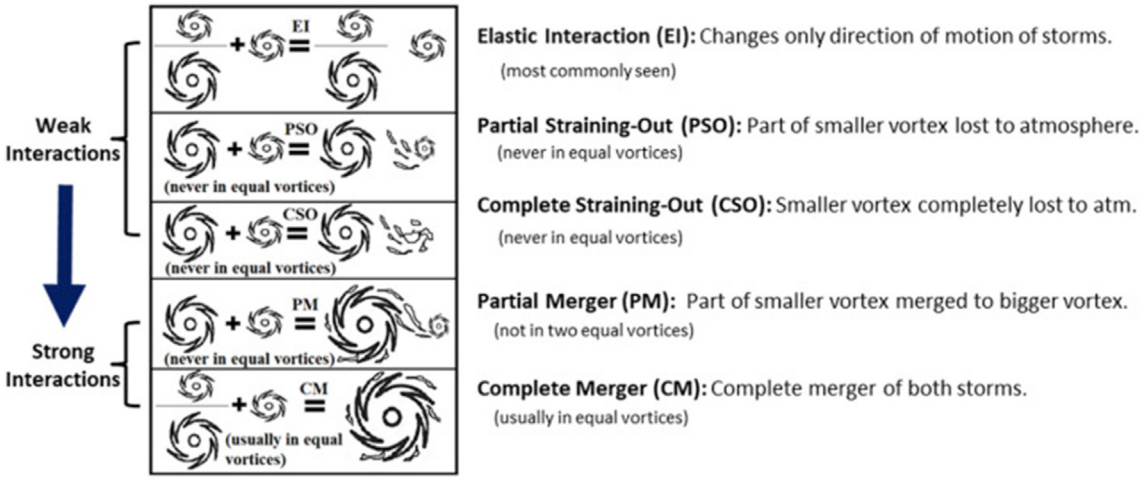

Fig. 7. Schematic diagram of the Fujiwhara effect. From Fig. 1 of Liou and Pandey (2020).

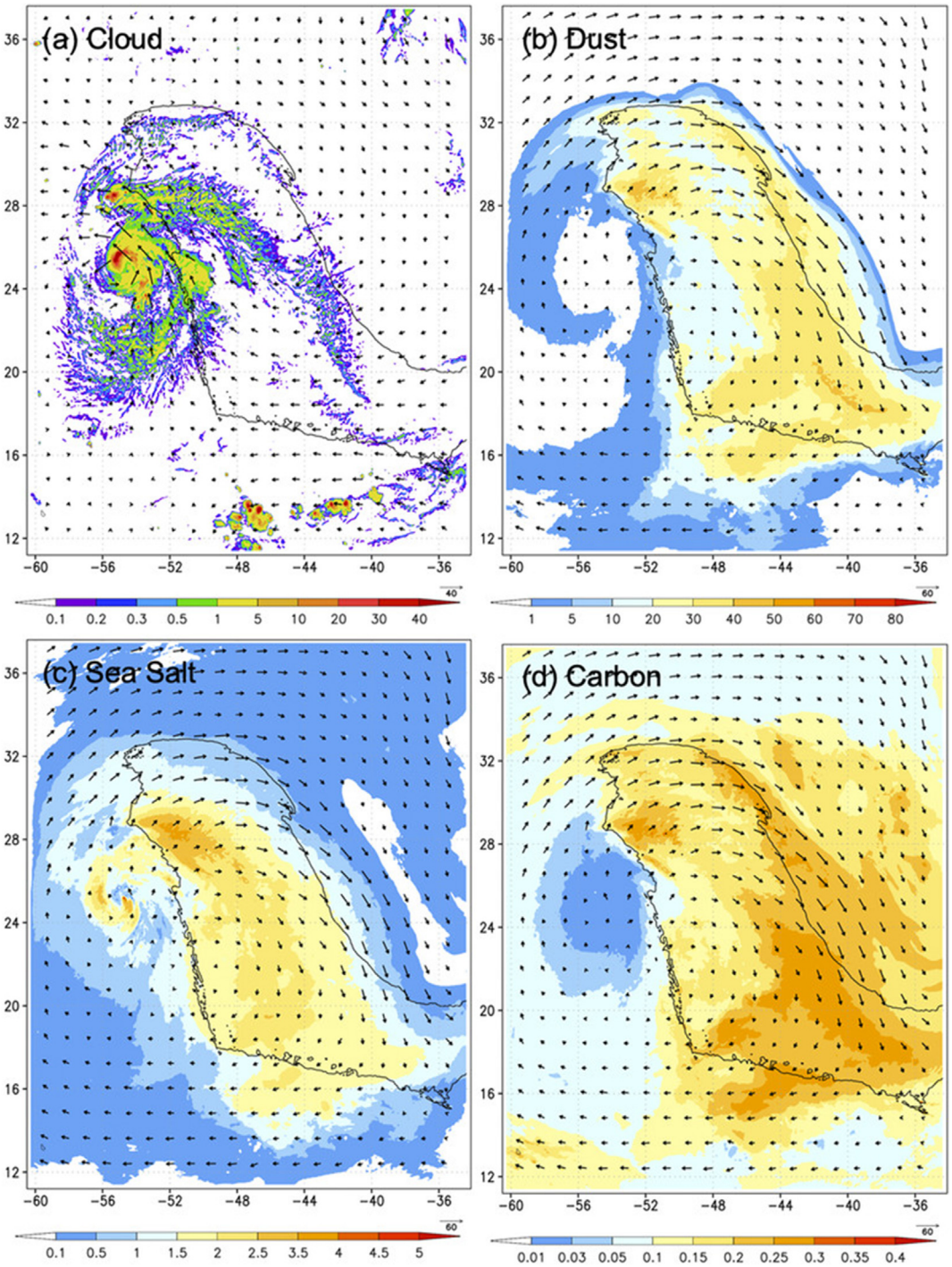

Fig. 8. Simulated horizontal distributions (shading) of 300–100-hPa layer-averaged (a) cloud (ice + snow + graupel) mixing ratio (0.01 g kg^{-1}), (b) dust mixing ratio (μg kg^{-1}), (c) sea salt mixing ratio (μg kg^{-1}), and (d) black and organic carbon mixing ratio (μg kg^{-1}). The black contour shows the aerosol optical depth = 0.2 threshold. Vectors in (a) show 900-hPa winds; in (b)–(d), vectors indicate 200-hPa winds. From Fig. 12 of Shi et al. (2021).

intensity. Liang et al. (2021a) found that dust weakened the simulated intensity of Earl (2010) through radiative stabilization. Reed et al. (2019) concluded that more dust resulted in lower lifetime maximum intensity and accumulated cyclone energy in a climate model simulation. Interestingly, Huang et al. (2020) found that simply having a large aerosol optical depth, signaling a dusty airmass, around a TC was not well associated with a lack of intensification. Rather, non-intensifying TCs interacting with the SAL have greater VWS and drier air. Furthermore, the effects of the SAL may depend on the TC lifecycle stage, having net detrimental effects on intensity in the tropical depression stage and net positive effects in the hurricane stage via effects on cloud ice (Luo and Han 2021; Fig. 9).

5.3. Effects of radiation

There is a growing understanding of radiative effects on TCs. Cloud-radiative feedbacks (CRFs), associated with interactions of cloud ice and longwave radiation, are important for accelerating intensification (Wing 2022), particularly early in development when the radiative heating anomalies are concentrated within the radius of maximum wind in the low-to-mid troposphere. Longwave CRF may hasten rapid intensification onset (Ruppert et al., 2020; Fig. 10) by increasing inner-core moist static energy (Chen et al., 2019a). Modeling results are supported by satellite observations of intensifying TCs having greater radiative flux convergence due to clouds compared to weakening TCs (Wu et al., 2021).

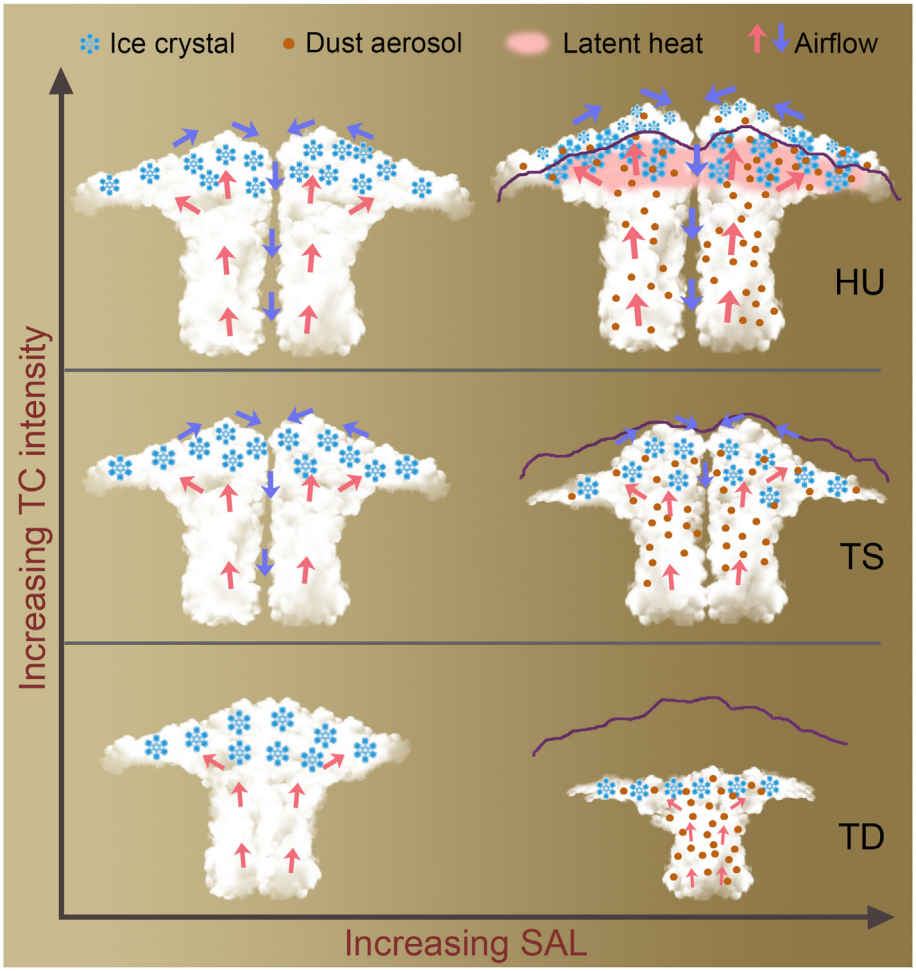

Fig. 9. Conceptual summary of SAL effects on TC cloud systems as a function of SAL strength and TC intensity. The purple curves are the cloud-top heights under pristine conditions. From Fig. 13 of Luo and Han (2021).

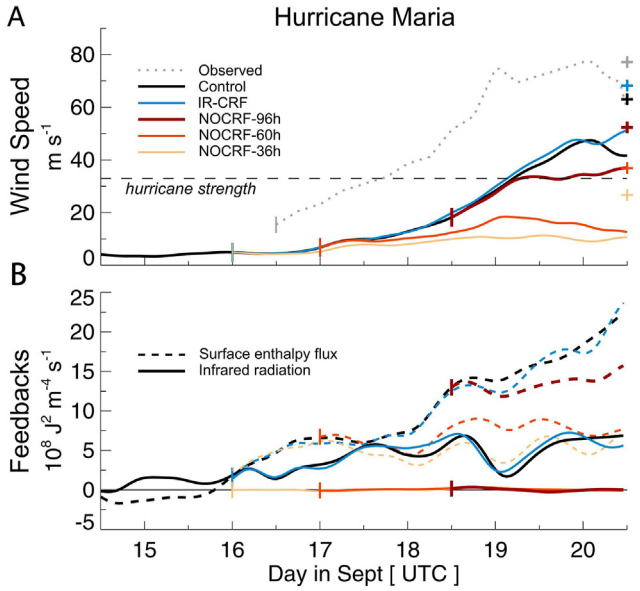

Fig. 10. Time series of (a) intensity and (b) frozen moist static energy (MSE) feedback terms due to external (diabatic) sources: surface enthalpy flux (dashed) and infrared radiation (solid) for a set of simulations of Maria (2017). Cloud–radiation interaction is turned off at times indicated by the vertical ticks (in IR-CRF, cloud–infrared radiation interaction is retained). Abscissa crosses denote maximum wind speed values without azimuthal averaging. From Fig. 2a and c of Ruppert et al. (2020).

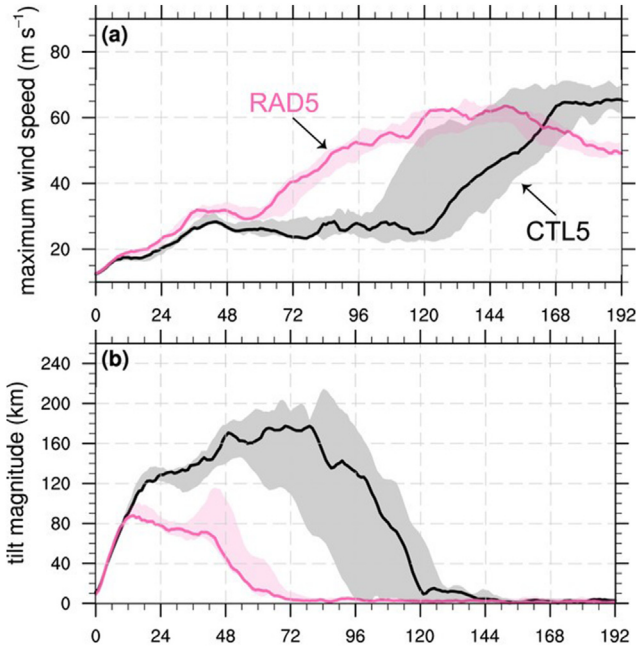

Fig. 11. Time series of hourly (a) intensity and (b) 400–900-hPa tilt magnitude from an ensemble of simulations without radiation (CTL5; black and gray) and with the Rapid Radiative Transfer Model for GCMs (RTMG) (referred to as RAD5; pink), both with 5 m s^{-1} shear. Lines represent the unperturbed member from each ensemble; shading extends from ensemble minimum to ensemble maximum at each hour. A 6-h running mean was applied to each time series. From Fig. 2a and b of Rios-Berrios (2020).

The effects of diurnally varying and constant radiation on TCs have been further explored. Idealized simulations that impose a "constant night" intensify more quickly than those that impose a "constant day" (Tang et al., 2019; Trabing et al., 2019), but the shortwave flux imposed in the constant-day simulations might matter (Wing 2022). In a constant night setup, radiative cooling rates at the storm top and effects on the secondary circulation are important (Trabing et al., 2019).

The effects of radiation may also make TCs more resilient to VWS through cooling and moistening the TC environment, which weakens downdraft activity and cold pool strength (Rios-Berrios 2020). In an ensemble of idealized simulations with radiation, Rios-Berrios (2020) found a faster reduction of tilt, earlier intensification, and less spread in the intensity evolution compared to simulations without radiation (Fig. 11).

6. TC intensity change during landfalls

6.1. Post-landfall intensity decay

The general response of TC intensity to landfall can be simply related to reduced surface entropy fluxes. Chen and Chavas (2020) explained the distinct mechanisms for different intensity responses of an idealized axisymmetric mature TC to modified major surface conditions (Fig. 12). They found that surface drying induced a single dominant intensity response. The primary TC circulation gradually weakens within the inner core in response to the gradual eyewall stabilization due to the rapid reduction in surface moisture fluxes. In contrast, surface roughening induces TC intensity responses on two distinct timescales. The TC first decays rapidly as the primary circulation is nearly instantaneously weakened due to the direct enhancement of the angular momentum sink from surface friction. Meanwhile, the secondary circulation is temporarily enhanced due to the strengthened frictionally induced inflow despite the thermodynamic eyewall stabilization. Afterward, the TC gradually decays till the end of the evolution as the eyewall stabilization gradually weakens the entire overturning circulation. Additionally, the time-dependent response of TC intensity to combined surface drying and roughening can be predicted as the product of the responses to each forcing (Chen and Chavas 2021). Hlywiak and Nolan

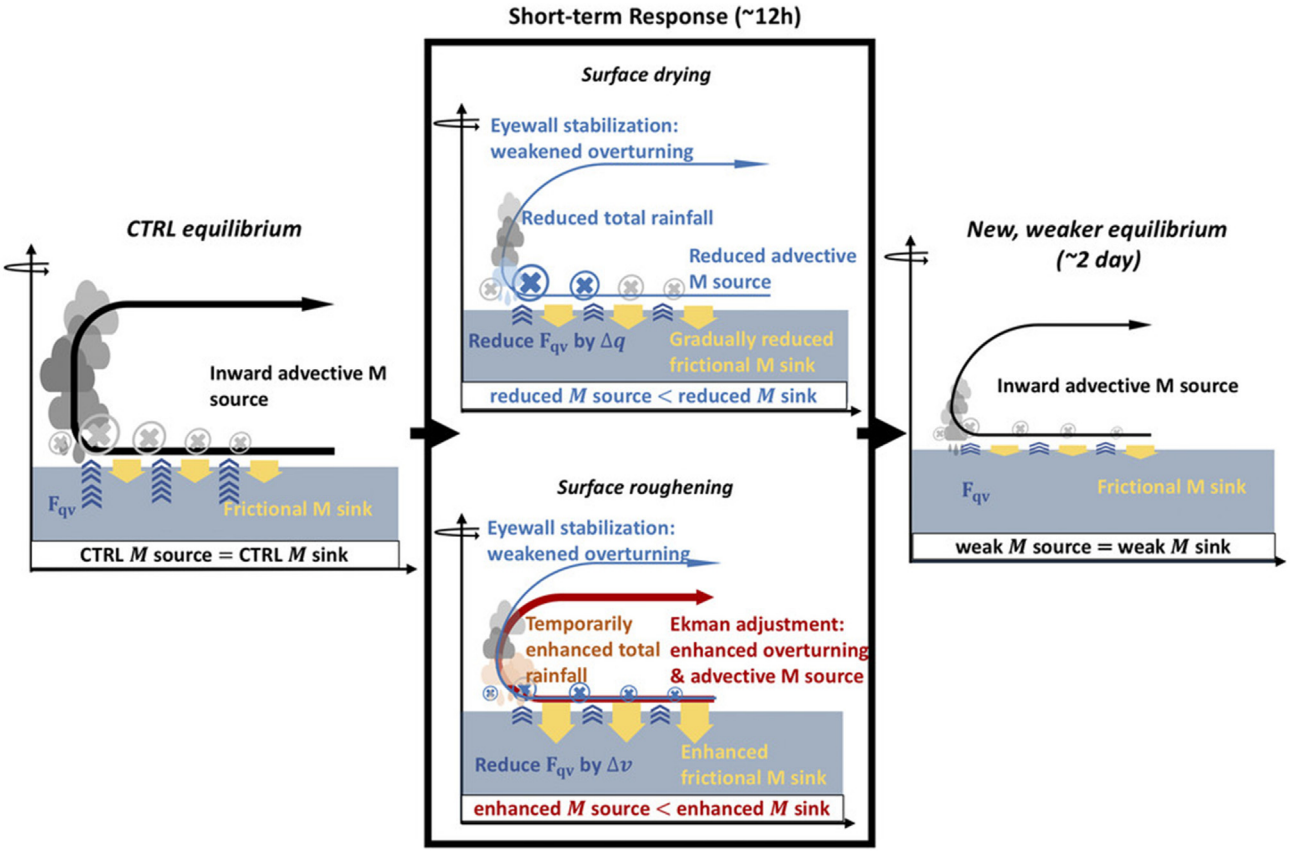

Fig. 12. A conceptual schematic of the short-term response and long-term re-equilibration to surface roughening or drying. The schematic shows primary circulation (crosses) and overturning circulation and depicts responses to surface moisture fluxes F_{qv}, angular momentum (M) sources and sinks, and precipitation. The response magnitude of each quantity is indicated by the icon width or size, with an enhancement or reduction colored red or blue, respectively. Figure 17 of Chen and Chavas (2020).

(2021) also suggested that intensity decay was initially more sensitive to surface roughness (roughness length Z_0) than soil moisture (volumetric soil water content Sc), especially for the most intense wind. Each forcing affects TC decay within different radii and storm-relative quadrants. The sensitivity to each forcing depends on TC strength and size (Fig. 13). The sensitivity to each forcing also depends on TC strength and size. Their results further suggested that the negative feedback between soil moisture and surface temperatures was an essential control on inland intensity since increasingly negative sensible heat fluxes would counter stronger latent heat fluxes.

6.2. Maintained intensity after landfall

In contrast to a rougher and drying land surface that generally weakens the storm, saturated soils or shallow waters provide inland TCs additional external moist enthalpy to maintain their structure and intensity. A series of recent Brown Ocean effects (BOE) studies (Yoo et al., 2020, 2021; Shepherd et al., 2021) explored the contribution of sandy soil to the frequent TC maintenance and re-intensification after TC landfall. Though intensity sensitivities can be recognized among experiments varying soil moisture, flux, and texture conditions, their results indicate that the BOE is not a binary influence on TC intensity (Fig. 14). Thus, the BOE influences on TC intensity after landfall remain an open question. Considering the rarity and complexity of maintained and re-intensified TCs after landfall, Thomas and Shepherd (2022) introduced a machine-learning method to examine the TC record to improve the climatological representation of such cases, further confirming the role of warm and moist soil on TC inland intensity.

6.3. Post-landfall TC intensity change models

Advanced theories describing the time-dependent TC intensification have been formulated based on TC

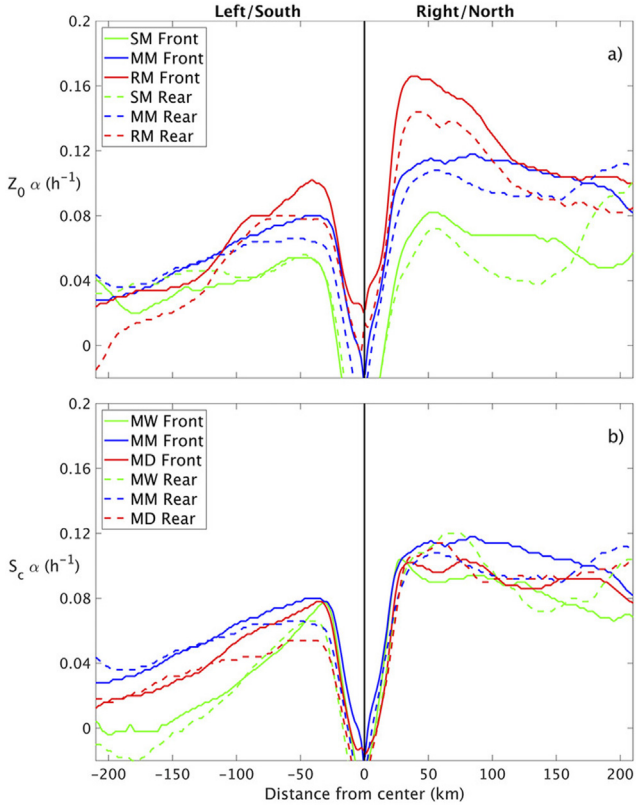

Fig. 13. The e-folding time decay constant a(r) (h^{-1}) for (a) smooth (green), moderate (blue), and rough (red) surface with moderate soil water content, and (b) moderate surface roughness with wet (green), moderate (blue), and dry soil water content by TC quadrant. Here Z_0 and S_c are the surface roughness lenth and moisture content, respectively. Positive (negative) radii show the right (left)-of-motion quadrant-averaged S10, and solid (dashed) lines indicate the front (rear) quadrants. The TC is moving into the page in this frame of reference. Fig. 9 of Hlywiak and Nolan (2021).

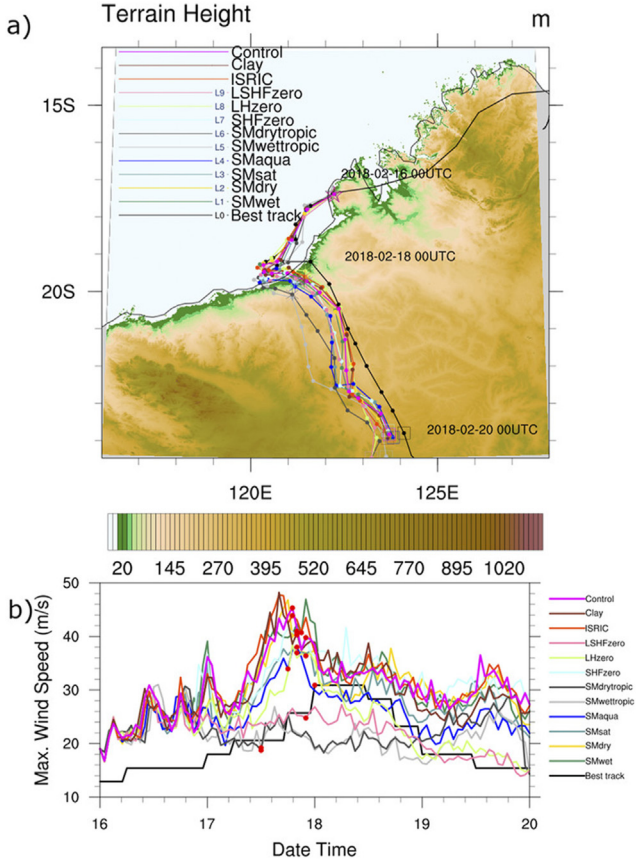

Fig. 14. (a) Six-hourly track analysis composite of TC Kelvin simulations superimposed over the model terrain height in the land/soil moisture perturbation study and (b) time series of hourly maximum wind speed. Labels in legend are consistent with simulation IDs in Table 1 of Yoo et al., (2020). The black line represents the observed track of Kelvin by the BoM (here, labeled as ''best track''). Storm's 6-hourly center locations of the best track were plotted with filled circles only for the simulation period (16–20 Feb 2018). The initial (final) locations of the simulated storm centers are marked with stars (squares) along with their annotations for the times. Red dots in (b) represent the time when the storm moved from ocean to land (i.e., landfall). Fig. 3 of Yoo et al. (2020).

thermodynamics over the ocean (Emanuel, 2012; Wang et al., 2021); however, they have not been tested against the intensity decaying process. To examine the extent to which the current intensity change theory can explain the inland TC intensity change, Chen and Chavas (2021) generalized the Emanuel (2012) intensification theory to predict the first-order TC intensity change decay in response to idealized landfalls from any non-zero initial intensity to a weak, final equilibrium intensity. This physics-based model can predict the first-order time-dependent weakening response of an idealized TC for any combination of drying and roughening and compares well with the prevailing empirical intensity decay model (Jing and Lin 2019). Phillipson and Toumi (2021) also derived a simple TC intensity decay model by modifying the frictional turbulent drag accounting for the partial to complete change in land roughness. The model fits an algebraic decay with a parameter determined by the ratio of the surface drag coefficient to the effective vortex depth. Considering the complexity of measuring the TC intensity change by the maximum wind speed, Sparks and Toumi (2022) also introduced a model of tropical cyclone central pressure filling at landfall, providing another avenue to predict the TC inland intensity change.

7. Summary and conclusions

This report synthesizes the research advances regarding the influences of external factors on TC intensity change over the past four years (2019–2022). The external forcing in focus includes the ocean, air-sea interaction, VWS, upper-level troughs, monsoon gyres, aerosols, the Saharan air layer, radiation, land surfaces, and others. New findings continue to come in, indicating encouraging progress in the past four years in examining the external factors influencing TC intensity change.

Studies of ocean effects note that salinity-stratification plays an important role in TC intensity change, and RW events tend to arise in regions with a stronger meridional SST gradient and cooler SSTs. In addition, increasing SSTs (e.g., over warm oceanic eddies) and air-sea moisture differences can efficiently increase surface heat fluxes, favoring TC intensification. New ocean observational platforms are also being constructed and operated in succession, furnishing more comprehensive and

abundant ocean observational data to improve the observational and forecasting techniques of physical processes of TC intensity change.

Studies of VWS effects show that the onset of more rapid rates of TC intensification is closely linked to the transition of a misaligned TC toward alignment, but complete alignment seems not to be a requirement for RI. VWS-induced ventilation can be divided into radial and downdraft pathways, and they both transport low-θ_e air to the TC circulation, significantly influencing TC intensity. In addition, the TC intensity change caused by VWS responds to TC intensity, vortex structure, and shear properties. Some unique structures of the TC circulation can also modulate environmental VWS; for instance, blocking due to upper-level outflow from the TC can locally decrease VWS and, thus, facilitate TC intensification.

The understanding of interactions between the TC and ambient systems and the associated impacts on TC intensity change has been further deepened over the past four years. Enhanced TC-trough interactions are critical for RI in some TC cases because of strengthened warm air advection, but upper-level troughs tend to limit TC intensification in other cases because of dry midlevel air intrusions and increased VWS. In addition, monsoon troughs can enhance low-level convergence, water vapor penetration, and vorticity in the inner-core region of TCs, leading to TC intensification.

Aerosol, SAL, and radiation effects on TC intensity change are further unearthed. The radiation absorption by aerosols can change temperature profiles and affect rainbands due to changes in stability and microphysics. Sea spray and sea salt aerosols may cause an increase in cloud ice, precipitation, latent heating, and vertical velocity in TC's inner core. The SAL is indicated to have net detrimental effects on TC intensity in the tropical depression stage and net positive effects in the hurricane stage. Additionally, longwave CRF may accelerate rapid intensification onset. The effects of radiation may also make TCs more resilient to VWS, along with a faster reduction of vortex tilt and earlier intensification.

The intensity change of TCs after landfall is also receiving increasing interest. TC intensity decay is initially more sensitive to surface roughness than soil moisture. Afterward, the TC's inner core gradually weakens due to the rapid reduction in surface moisture fluxes. However, in some post-landfall cases, the BOE can provide inland TCs additional moist enthalpy to maintain their intensity. Also, physics-based models are developed to predict the time-dependent weakening response of post-landfall TC intensity decay, considering drying and roughening effects.

Acknowledgement

The constructive comments by three anonymous reviewers and the Editor are greatly appreciated and are valuable in improving the manuscript. This work was jointly supported by the National Natural Science Foundation of China under Grant Nos. 42175005 and 41875054.

References

Alland, J.J., Davis, C.A., 2022. Effects of surface fluxes on ventilation pathways and the intensification of Hurricane Michael (2018). J. Atmos. Sci. 79, 1211–1229. https://doi.org/10.1175/JAS-D-21-0166.1.

Alland, J.J., Tang, B.H., Corbosiero, K.L., Bryan, G.H., 2021a. Combined effects of midlevel dry air and vertical wind shear on tropical cyclone development. Part I: downdraft ventilation. J. Atmos. Sci. 78, 763–782. https://doi.org/10.1175/JAS-D-20-0054.1.

Alland, J.J., Tang, B.H., Corbosiero, K.L., Bryan, G.H., 2021b. Combined effects of midlevel dry air and vertical wind shear on tropical cyclone development. Part II: radial ventilation. J. Atmos. Sci. 78, 783–796. https://doi.org/10.1175/JAS-D-20-0055.1.

Alvey III, G.R., Zipser, E., Zawislak, J., 2020. How does Hurricane Edouard (2014) evolve toward symmetry before rapid intensification? A high-resolution ensemble study. J. Atmos. Sci. 77, 1329–1351. https://doi.org/10.1175/JAS-D-18-0355.1.

Alvey III, G.R., Fischer, M., Reasor, P., Zawislak, J., Rogers, R., 2022. Observed processes underlying the favorable vortex repositioning early in the development of Hurricane Dorian (2019). Mon. Wea. Rev. 150, 193–213. https://doi.org/10.1175/MWR-D-21-0069.1.

Balaguru, K., Patricola, C.M., Hagos, S.M., Leung, L.R., Dong, L., 2020a. Enhanced predictability of eastern North Pacific tropical cyclone activity using the ENSO Longitude Index. Geophys. Res. Lett. 47, e2020GL088849. https://doi.org/10.1029/2020GL088849.

Balaguru, K., Foltz, G.R., Leung, L.R., Kaplan, J., Xu, W., Reul, N., Chapron, B., 2020b. Pronounced impact of salinity on rapidly intensifying tropical cyclones. Bull. Amer. Meteorol. Soc. 101, E1497–E1511. https://doi.org/10.1175/BAMS-D-19-0303.1.

Boehm, A.M., Bell, M.M., 2021. Retrieved thermodynamic structure of Hurricane Rita (2005) from airborne multi-Doppler radar data. J. Atmos. Sci. 78, 1583–1605. https://doi.org/10.1175/JAS-D-20-0195.1.

Callaghan, J., 2019. The interaction of Hurricane Michael with an upper trough leading to intensification right up to landfall. Trop. Cyclone. Res. Rev. 8, 95–102. https://doi.org/10.6057/2019TCRR02.04.

Chen, B., Davis, C.A., Kuo, Y., 2019a. An idealized numerical study of shear-relative low-level mean flow on tropical cyclone intensity and size. J. Atmos. Sci. 76, 2309–2334. https://doi.org/10.1175/MWR-D-21-0120.1.

Chen, B., Davis, C.A., Kuo, Y., 2021a. Examination of the combined effect of deep-layer vertical shear direction and lower-tropospheric mean flow on tropical cyclone intensity and size based on the ERA5 reanalysis. Mon. Wea. Rev. 149, 4057–4076. https://doi.org/10.1175/JAS-D-18-0315.1.

Chen, J., Chavas, D.R., 2020. The transient responses of an axisymmetric tropical cyclone to instantaneous surface roughening and drying. J. Atmos. Sci. 77, 2807–2834. https://doi.org/10.1175/JAS-D-19-0320.1.

Chen, J., Chavas, D.R., 2021. Can existing theory predict the response of tropical cyclone intensity to idealized landfall? J. Atmos. Sci. 78, 3281–3296. https://doi.org/10.1175/JAS-D-21-0037.1.

Chen, X., Zhang, J.A., Marks, F.D., 2019b. A thermodynamic pathway leading to rapid intensification of tropical cyclones in shear. Geophys. Res. Lett. 46, 9241–9251. https://doi.org/10.1029/2019GL083667.

Chen, X., Gu, J., Zhang, J.A., Marks, F.D., Rogers, R.F., Cione, J.J., 2021b. Boundary layer recovery and precipitation symmetrization preceding rapid intensification of tropical cyclones under shear. J. Atmos. Sci. 78, 1523–1544. https://doi.org/10.1175/JAS-D-20-0252.1.

Cotton, W.R., Walko, R., 2021a. A modeling investigation of the potential impacts of pollution aerosols on Hurricane Harvey. J. Atmos. Sci. 78, 2323–2338. https://doi.org/10.1175/JAS-D-20-0076.1.

Cotton, W.R., Walko, R., 2021b. Examination of aerosol-induced convective invigoration using idealized simulations. J. Atmos. Sci. 78, 287–298. https://doi.org/10.1175/JAS-D-20-0023.1.

Dai, Y., Majumdar, S.J., Nolan, D.S., 2021. Tropical cyclone resistance to strong environmental shear. J. Atmos. Sci. 78, 1275–1293. https://doi.org/10.1175/JAS-D-20-0231.1.

DeMaria, M., 1996. The effect of vertical shear on tropical cyclone intensity change. J. Atmos. Sci. 53, 2076–2088. https://doi.org/10.1175/1520-0469(1996)053<2076:TEOVSO>2.0.CO;2.

Domingues, R., Kuwano-Yoshida, A., Chardon-Maldonado, P., Todd, R.E., Halliwell, G., Kim, H.S., Lin, I.I., Sato, K., Narazaki, T., Shay, L.K., Miles, T., 2019. Ocean observations in support of studies and forecasts of tropical and extratropical cyclones. Front. Mar. Sci. 6, 446. https://doi.org/10.3389/fmars.2019.00446.

Emanuel, K.A., 2012. Self-stratification of tropical cyclone outflow. Part II: implications for storm intensification. J. Atmos. Sci. 69, 988–996. https://doi.org/10.1175/JAS-D-11-0177.1.

Finocchio, P.M., Rios-Berrios, R., 2021. The intensity- and size-dependent response of tropical cyclones to increasing vertical wind shear. J. Atmos. Sci. 78, 3673–3690. https://doi.org/10.1175/JAS-D-21-0126.1.

Fischer, M.S., Tang, B.H., Corbosiero, K.L., 2019. A climatological analysis of tropical cyclone rapid intensification in environments of upper-tropospheric troughs. Mon. Wea. Rev. 147, 3693–3719. https://doi.org/10.1175/MWR-D-19-0013.1.

Fischer, M.S., Reasor, P.D., Rogers, R.F., Gamache, J.F., 2022. An analysis of tropical cyclone vortex and convective characteristics in relation to storm intensity using a Novel Airborne Doppler radar database. Mon. Wea. Rev. 150, 2255–2278. https://doi.org/10.1175/MWR-D-21-0223.1.

Gu, J., Tan, Z., Qiu, X., 2019. Intensification variability of tropical cyclones in directional shear flows: vortex tilt–convection coupling. J. Atmos. Sci. 76, 1827–1844. https://doi.org/10.1175/JAS-D-18-0282.1.

Hazelton, A.T., Zhang, X., Ramstrom, W., Gopalakrishan, S., Marks, F.D., Zhang, J.A., 2020. High-resolution ensemble HFV3 forecasts of Hurricane Michael (2018): rapid intensification in shear. Mon. Wea. Rev. 148, 2009–2032. https://doi.org/10.1175/MWR-D-19-0275.1.

Hlywiak, J., Nolan, D.S., 2019. The influence of oceanic barrier layers on tropical cyclone intensity as determined through idealized, coupled numerical simulations. J. Phys. Oceanogr. 49, 1723–1745. https://doi.org/10.1175/jpo-d-18-0267.1.

Hlywiak, J., Nolan, D.S., 2021. The response of the near-surface tropical cyclone wind field to inland surface roughness length and soil moisture content during and after landfall. J. Atmos. Sci. 78, 983–1000. https://doi.org/10.1175/JAS-D-20-0211.1.

Huang, W.T.K., Poberaj, C.S., Enz, B., Horat, C., Lohmann, U., 2020. When does the Saharan air layer impede the intensification of tropical cyclones? J. Clim. 33, 10609–10626. https://doi.org/10.1175/JCLI-D-19-0854.1.

Jaimes de la Cruz, B., Shay, L.K., Wadler, J.B., Rudzin, J.E., 2021. On the hyperbolicity of the bulk air-sea heat flux functions: insights into the efficiency of air-sea moisture disequilibrium for tropical cyclone intensification. Mon. Wea. Rev. 149, 1517–1534. https://doi.org/10.1175/MWR-D-20-0324.1.

Jiang, B., Lin, W., Li, F., Chen, B., 2019. Simulation of the effects of sea-salt aerosols on cloud ice and precipitation of a tropical cyclone. Atmos. Sci. Lett. 20, e936. https://doi.org/10.1002/asl.936.

Jing, R., Lin, N., 2019. Tropical cyclone intensity evolution modeled as a dependent hidden Markov process. J. Clim. 32, 7837–7855. https://doi.org/10.1175/JCLI-D-19-0027.1.

Kumar, A.U., Brüggemann, N., Smith, R.K., Marotzke, J., 2021. Response of a tropical cyclone to a subsurface ocean eddy and the role of boundary layer dynamics. Quart. J. Roy. Meteorol. Soc. 148, 378–402. https://doi.org/10.1002/qj.4210.

Lee, T., Wu, C., Rios-Berrios, R., 2021. The role of low-level flow direction on tropical cyclone intensity changes in a moderate-sheared environment. J. Atmos. Sci. 78, 2859–2877. https://doi.org/10.1175/JAS-D-20-0360.1.

Leipper, D., Volgenau, D., 1972. Hurricane heat potential of the Gulf of Mexico. J. Phys. Oceanogr. 2, 218–224. https://doi.org/10.1175/1520-0485(1972)002<0218:HHPOTG>2.0.CO;2.

Li, L., Ge, X., 2021. Intensity change of Noru (2017) during binary tropical cyclones interaction. Asia-pac J. Atmos. Sci. 57, 135–147. https://doi.org/10.1007/s13143-020-00181-7.

Liang, J., Chen, Y., Arellano, A.F., Mamun, A.A., 2021a. Model sensitivity study of the direct radiative impact of Saharan dust on the early stage of Hurricane Earl. Atmosphere 12, 1181. https://doi.org/10.3390/atmos12091181.

Liang, Z., Ding, J., Fei, J., Cheng, X., Huang, X., 2021b. Direct/indirect effects of aerosols and their separate contributions to Typhoon Lupit (2009): eyewall versus peripheral rainbands. Sci. China Earth Sci. 64, 2113–2128. https://doi.org/10.1007/s11430-020-9816-7.

Liou, Y.-A., Pandey, R.S., 2020. Interactions between typhoons parma and melor (2009) in North west pacific ocean. Weather. Clim. Extremes 29, 100272. https://doi.org/10.1016/j.wace.2020.100272.

Liu, H.-Y., Wang, Y., Gu, J.-F., 2021. Intensity change of binary tropical cyclones (TCs) in idealized numerical simulations: two identical mature TCs. J. Atmos. Sci. 78, 1001–1020. https://doi.org/10.1175/JAS-D-20-0116.1.

Luo, H., Han, Y., 2021. Impacts of the Saharan air layer on the physical properties of the Atlantic tropical cyclone cloud systems: 2003–2019. Atmos. Chem. Phys. 21, 15171–15184. https://doi.org/10.5194/acp-21-15171-2021.

Luo, H., Jiang, B., Li, F., Lin, W., 2019. Simulation of the effects of sea-salt aerosols on the structure and precipitation of a developed tropical cyclone. Atmos. Res. 217, 120–127. https://doi.org/10.1016/j.atmosres.2018.10.018.

Ma, Z., Fei, J., Huang, X., 2019. A definition of rapid weakening for tropical cyclones over the western North Pacific. Geophys. Res. Lett. 46, 11471–11478. https://doi.org/10.1029/2019GL085090.

Miles, T.N., Zhang, D., Foltz, G.R., Zhang, J., Meinig, C., Bringas, F., Triñanes, J., Le Hénaff, M., Aristizabal Vargas, M.F., Coakley, S., Edwards, C.R., Gong, D., Todd, R.E., Oliver, M.J., Wilson, W.D., Whilden, K., Kirkpatrick, B., Chardon-Maldonado, P., Morell, J.M., Hernandez, D., Kuska, G., Stienbarger, C.D., Bailey, K., Zhang, C., Glenn, S.M., Goni, G.J., 2021. Uncrewed ocean gliders and saildrones support hurricane forecasting and research. In: Kappel, E.S., Juniper, S.K., Seeyave, S., Smith, E., Visbeck, M. (Eds.), *Frontiers In Ocean Observing: Documenting Ecosystems, Understanding Environmental Changes, Forecasting Hazards*. 78–81. A Supplement to Oceanography. https://doi.org/10.5670/oceanog.2021.supplement.02-28, 34.

Nguyen, L.T., Rogers, R., Zawislak, J., Zhang, J.A., 2019. Assessing the influence of convective downdrafts and surface enthalpy fluxes on tropical cyclone intensity change in moderate vertical wind shear. Mon. Wea. Rev. 147, 3519–3534. https://doi.org/10.1175/MWR-D-18-0461.1.

Nolan, D.S., Moon, Y., Stern, D.P., 2007. Tropical cyclone intensification from asymmetric convection: energetics and efficiency. J. Atmos. Sci. 64, 3377–3405. https://doi.org/10.1175/JAS3988.1.

Phillipson, L.M., Toumi, R., 2021. A physical interpretation of recent tropical cyclone post-landfall decay. Geophys. Res. Lett. 48, e2021GL094105. https://doi.org/10.1029/2021GL094105.

Potter, H., DiMarco, S.F., Knap, A.H., 2019. Tropical cyclone heat potential and the rapid intensification of Hurricane Harvey in the Texas Bight. J. Geophys. Res. Oceans 124, 2440–2451. https://doi.org/10.1029/2018JC014776.

Qin, N., Wu, L., 2021. Possible environmental influence on eyewall expansion during the rapid intensification of Hurricane Helene (2006). Front. Earth Sci. 9, 715012. https://doi.org/10.3389/feart.2021.715012.

Qiu, W., Wu, L., Ren, F., 2020. Monsoonal influences on offshore rapid intensification of landfalling typhoons in a sheared environment over the South China Sea. Wea. Forecast. 35, 623–634. https://doi.org/10.1175/WAF-D-19-0134.1.

Reed, K.A., Bacmeister, J.T., Huff, J.J.A., Wu, X., Bates, S.C., Rosenbloom, N.A., 2019. Exploring the impact of dust on North Atlantic hurricanes in a high-resolution climate model. Geophys. Res. Lett. 46, 1105–1112. https://doi.org/10.1029/2018GL080642.

Rios-Berrios, R., 2020. Impacts of radiation and cold pools on the intensity and vortex tilt of weak tropical cyclones interacting with vertical wind shear. J. Atmos. Sci. 77, 669–689. https://doi.org/10.1175/JAS-D-19-0159.1.

Rogers, R.F., Reasor, P.D., Zawislak, J.A., Nguyen, L.T., 2020. Precipitation processes and vortex alignment during the intensification of a weak tropical cyclone in moderate vertical shear. Mon. Wea. Rev. 148, 1899–1929. https://doi.org/10.1175/MWR-D-19-0315.1.

Rudzin, J.E., Shay, L.K., Jaimes de la Cruz, B., 2019. The impact of the Amazon–Orinoco River plume on enthalpy flux and air–sea Interaction within Caribbean Sea tropical cyclones. Mon. Wea. Rev. 147, 931–950. https://doi.org/10.1175/MWR-D-18-0295.1.

Rudzin, J.E., Chen, S., Sanabia, E.R., Jayne, S.R., 2020. The air-sea response during Hurricane Irma's (2017) rapid intensification over the Amazon-

Orinoco River plume as measured by atmospheric and oceanic observations. J. Geophys. Res. Atmos. 125, e2019JD032368. https://doi.org/10.1029/2019JD032368.

Ruppert, J.H., Wing, A.A., Tang, X., Duran, E.L., 2020. The critical role of cloud–infrared radiation feedback in tropical cyclone development. Proc. Natl. Acad. Sci. 117, 27884–27892. https://doi.org/10.1073/pnas.2013584117.

Ryglicki, D.R., Velden, C.S., Reasor, P.D., Hodyss, D., Doyle, J.D., 2021. Observations of atypical rapid intensification characteristics in Hurricane Dorian (2019). Mon. Wea. Rev. 149, 2131–2150. https://doi.org/10.1175/MWR-D-20-0413.1.

Ryglicki, D.R., Hodyss, D., Rainwater, G., 2020. The tropical cyclone as a divergent source in a background flow. J. Atmos. Sci. 77, 4189–4210. https://doi.org/10.1175/JAS-D-20-0030.1.

Ryglicki, D.R., Doyle, J.D., Hodyss, D., Cossuth, J.H., Jin, Y., Viner, K.C., Schmidt, J.M., 2019. The unexpected rapid intensification of Tropical Cyclones in moderate vertical wind shear. Part III: outflow–environment interaction. Mon. Wea. Rev. 147, 2919–2940. https://doi.org/10.1175/MWR-D-18-0370.1.

Schecter, D.A., 2022. Intensification of tilted tropical cyclones over relatively cool and warm oceans in idealized numerical simulations. J. Atmos. Sci. 79, 485–512. https://doi.org/10.1175/JAS-D-21-0051.1.

Schecter, D.A., Menelaou, K., 2020. Development of a misaligned tropical cyclone. J. Atmos. Sci. 77, 79–111. https://doi.org/10.1175/JAS-D-19-0074.1.

Shay, L.K., Goni, G.J., Black, P.G., 2000. Effects of a warm oceanic feature on Hurricane Opal. Mon. Wea. Rev. 128, 1366–1383. https://doi.org/10.1175/1520-0493(2000)128<1366:EOAWOF>2.0.CO;2.

Shay, L.K., Brewster, J.K., Jaimes, B., Gordon, C., Fennel, K., Furze, P., Fargher, H., He, R., 2019. Physical and Biochemical Structure Measured by APEX-EM Floats. IEEE/OES. Twelfth Current, Waves and Turbulence Measurement (CWTM), San Diego, CA, USA, pp. 1–6. https://doi.org/10.1109/CWTM43797.2019.8955168.

Shepherd, J.M., Thomas, A.M., Santanello, J.A., Lawston-Parker, P., Basara, J., 2021. Evidence of warm core structure maintenance over land: a case study analysis of cyclone Kelvin. Environ. Res. 3, 045004. https://doi.org/10.1088/2515-7620/abf39a.

Shi, D., Chen, G., 2021. The implication of outflow structure for the rapid intensification of tropical cyclones under vertical wind shear. Mon. Wea. Rev. 149, 4107–4127. https://doi.org/10.1175/MWR-D-21-0141.1.

Shi, J.J., Braun, S.A., Tao, Z., Matsui, T., 2021. Influence of the saharan air layer on Hurricane Nadine (2012). Part I: observations from the hurricane and severe storm sentinel (HS3) investigation and modeling results. Mon. Wea. Rev. 149, 3541–3562. https://doi.org/10.1175/MWR-D-20-0344.1.

Shpund, J., Khain, A., Rosenfeld, D., 2019. Effects of sea spray on the dynamics and microphysics of an idealized tropical cyclone. J. Atmos. Sci. 76, 2213–2234. https://doi.org/10.1175/JAS-D-18-0270.1.

Song, J., Klotzbach, P.J., Duan, Y., Guo, H., 2020. Recent increase in tropical cyclone weakening rates over the western North Pacific. Geophys. Res. Lett. 47, e2020GL090337. https://doi.org/10.1029/2020GL090337.

Sparks, N., Toumi, R., 2022. A physical model of tropical cyclone central pressure filling at landfall. J. Atmos. Sci. 79, 2585–2599. https://doi.org/10.1175/JAS-D-21-0196.1.

Tang, B., Emanuel, K., 2010. Midlevel ventilation's constraint on tropical cyclone intensity. J. Atmos. Sci. 67, 1817–1830. https://doi.org/10.1175/2010JAS3318.1.

Tang, X., Tan, Z.-M., Fang, J., Munsell, E.B., Zhang, F., 2019. Impact of the diurnal radiation contrast on the contraction of radius of maximum wind during intensification of Hurricane Edouard (2014). J. Atmos. Sci. 76, 421–432. https://doi.org/10.1175/JAS-D-18-0131.1.

Tao, D., Zhang, F., 2019. Evolution of dynamic and thermodynamic structures before and during rapid intensification of tropical cyclones: sensitivity to vertical wind shear. Mon. Wea. Rev. 147, 1171–1191. https://doi.org/10.1175/MWR-D-18-0173.1.

Thomas, A.M., Shepherd, J.M., 2022. A Machine-Learning based tool for diagnosing inland tropical cyclone maintenance or intensification events. Front. Earth Sci. 10, 818671. https://doi.org/10.3389/feart.2022.818671.

Trabing, B.C., Bell, M.M., Brown, B.R., 2019. Impacts of radiation and upper-tropospheric temperatures on tropical cyclone structure and intensity. J. Atmos. Sci. 76, 135–153. https://doi.org/10.1175/JAS-D-18-0165.1.

Wadler, J.B., Nolan, D.S., Zhang, J.A., Shay, L.K., 2021a. Thermodynamic characteristics of downdrafts in Tropical Cyclones as seen in idealized simulations of different intensities. J. Atmos. Sci. 78, 3503–3524. https://doi.org/10.1175/MWR-D-20-0145.1.

Wadler, J.B., Zhang, J.A., Rogers, R.F., Jaimes, B., Shay, L.K., 2021b. The rapid intensification of Hurricane Michael (2018): storm structure and the relationship to environmental and Air–Sea interactions. Mon. Wea. Rev. 149, 245–267. https://doi.org/10.1175/MWR-D-20-0145.1.

Wadler, J.B., Cione, J.J., Zhang, J.A., Kalina, E.A., Kaplan, J., 2022. The effects of environmental wind shear direction on tropical cyclone boundary layer thermodynamics and intensity change from multiple observational datasets. Mon. Wea. Rev. 150, 115–134. https://doi.org/10.1175/MWR-D-21-0022.1.

Wang, Y., Li, Y., Xu, J., 2021. A new time-dependent theory of tropical cyclone intensification. J. Atmos. Sci. 78, 3855–3865. https://doi.org/10.1175/JAS-D-21-0169.1.

Wing, A.A., 2022. Acceleration of tropical cyclone development by cloud-radiative feedbacks. J. Atmos. Sci. 79, 2285–2305. https://doi.org/10.1175/JAS-D-21-0227.1.

Wu, S.-N., Soden, B.J., Nolan, D.S., 2021. Examining the role of cloud radiative interactions in tropical cyclone development using satellite measurements and WRF simulations. Geophys. Res. Lett. 48, e2021GL093259. https://doi.org/10.1029/2021GL093259.

Wu, Y., Chen, S., Li, W., Fang, R., Liu, H., 2020. Relative vorticity is the major environmental factor controlling tropical cyclone intensification over the Western North Pacific. Atmos. Res. 237, 104874. https://doi.org/10.1016/j.atmosres.2020.104874.

Yan, Z., Ge, X., Wang, Z., Wu, C.-C., Peng, M., 2021. Understanding the impacts of upper-tropospheric cold low on Typhoon Jongdari (2018) Using piecewise potential vorticity inversion. Mon. Wea. Rev. 149, 1499–1515. https://doi.org/10.1175/MWR-D-20-0271.1.

Yan, Z.Y., Ge, X., Peng, M., Li, T., 2019. Does monsoon gyre always favour tropical cyclone rapid intensification? Quart. J. Roy. Meteorol. Soc. 145, 2685–2697. https://doi.org/10.1002/qj.3586.

Yang, L., Luo, X., Chen, S., Zhou, X.-L., Wang, W.-Q., 2022. Characteristics of rapidly intensifying tropical cyclones in the South China Sea, 1980–2016. Adv. Clim. Changes Res. 13, 333–343. https://doi.org/10.1016/j.accre.2022.04.004.

Yoo, J., Santanello Jr., J.A., Shepherd, M., Kumar, S., Lawston, P., Thomas, A.M., 2020. Quantification of the land surface and Brown Ocean influence on tropical cyclone intensification over land. J. Hydrometeorol. 21, 1171–1192. https://doi.org/10.1175/JHM-D-19-0214.1.

Yoo, J., Santanello Jr., J.A., Shepherd, M., Kumar, S., Lawston, P., Wakefield, R., Thomas, A.M., 2021. Quantifying the Land Surface and Boundary Layer Influences on the Maintenance and Intensification of TS Bill (2015) Using the NASA Unified WRF Modeling System with a Lagrangian Backward Trajectory Analysis of the NOAA HYSPLIT Model. AGU Fall Meeting 2021, held in New Orleans, LA, 13-17 December 2021, id: H25L-1179. https://ui.adsabs.harvard.edu/abs/2021AGUFM.H25L1179Y.

Yue, L., Wang, Y., Zhou, J., Zhang, X., 2020. A comparative study on the effect of upstream trough on intensity changes of two types of tropical cyclones during extratropical transition. Asia-pac J. Atmos. Sci. 56, 131–146. https://doi.org/10.1007/s13143-019-00136-7.

Zhang, L., Oey, L., 2019. Young ocean waves favor the rapid intensification of tropical cyclones—a global observational analysis. Mon. Wea. Rev. 147, 311–328. https://doi.org/10.1175/MWR-D-18-0214.1.